RAA 2019 Vol. **19** No. **3**, 48(10pp) doi: 10.1088/1674–4527/19/3/48

http://www.raa-journal.org *http://iopscience.iop.org/raa*

***R**esearch in*
***A**stronomy and*
***A**strophysics*

A new method to determine the gravity field of small bodies from line-of-sight acceleration data

Nian-Chuan Jian[1], Jian-Guo Yan[2,3], Jin-Song Ping[4], Jean-Pierre Barriot[5] and J. Alexis P. Rodriguez[6]

[1] Shanghai Astronomical Observatory, Chinese Academy of Science, Shanghai 200030, China
[2] State Key Laboratory of Information Engineering in Surveying, Mapping and Remote Sensing, Wuhan University, Wuhan 430070, China; *jgyan@whu.edu.cn*
[3] Instituto de Astronomia y Ciencias Planetarias de Atacama, Universidad de Atacama, Copayapu 485, Chile
[4] National Astronomical Observatory of China, Chinese Academy of Science, Beijing 100101, China
[5] University of French Polynesia, Geodesy Observatory of Tahiti, Laboratoire GEPASUD, BP 6570, 98702 Faaa airport, Tahiti, French Polynesia
[6] Planetary Science Institute, 1700 East Fort Lowell Road, Suite 106, Tucson, AZ 85719-2395, USA

Received 2018 August 16; accepted 2018 September 28

Abstract We present a new method to derive line-of-sight acceleration observables from spacecraft radio tracking data. The observables can be used to estimate the mass and gravity of a natural satellite as a spacecraft flyby. The corresponding observation model adapts to one-way and two/three-way tracking modes. As a test case for method validation and application, we estimated the mass and degree two gravity field for the Martian moon Phobos using simulated tracking data when the spacecraft Mars Express flew by Phobos on 2013 December 29. We have a few real tracking data during flyby and they will be used to confirm raw data simulation. The main purpose of this paper is to demonstrate the method of line-of-sight acceleration reduction from raw tracking data and the feasibility to estimate mass and gravity of a natural satellite using this type of observable. This novel method is potentially applicable to planet and asteroid gravity field studies combined with Doppler tracking data.

Key words: line of sight acceleration — Doppler — celestial mechanics

1 INTRODUCTION

Line-of-sight (LOS) acceleration data have been used since the early stages of space exploration to derive local models of the gravity fields of the Moon and planets. Making use of the LOS acceleration generated from the radio tracking data of the Lunar Orbiter, Muller & Sjogren (1968) calculated the gravity anomaly distribution on the lunar nearside and thus first identified the lunar mascons. Barriot & Balmino (1992) were the first to generate a local gravity field model of Venus using LOS gravity data from Pioneer Venus Orbiter, and later on cycles 5 and 6 of the Magellan mission. More recently, based on two-way Doppler tracking data from the Lunar Prospector (LP) mission, Sugano & Heki (2004) derived the LOS acceleration values and produced a lunar nearside gravity anomaly map. Han (2008) deployed the spectrum method to generate a high-resolution lunar nearside gravity field model (up to degree and order 2000), based on similar LP LOS acceleration data. For the Chang'E-3 mission, Sun et al. (2013) also used LOS acceleration of LP mission to investigate the local gravity field structure of the Chang'E-3 landing site, Sinus Iridum. The LOS acceleration method mentioned in these papers builds on the algorithm developed for lunar mass concentrations by Muller & Sjogren (1968). This acceleration is actually "residual LOS acceleration" generated from a numerical differentiation (cubic-spline) of Doppler residuals. The "residual LOS acceleration" unveils local gravity anomalies in a celestial body, such as can be associated with lunar mass concentrations. The data processing method adopted was a standard observation type, Line of Sight Acceleration Profile Data Records (LOSAPDR) adopted in several deep space mis-

sions such as Magellan and the Lunar Prospector. The precision of Lunar Prospector LOSAPDR data is about several mgal, that is, in the magnitude of 10^{-5} m s^{-2} (Han 2008).

Instead of retrieving residual LOS acceleration values from Doppler data, we present a method to compute the "total LOS acceleration" directly from the raw tracking data. The total LOS acceleration method measures the instantaneous change rate of frequency at station using Taylor series fitting to raw data phase. The instantaneous change rate of frequency contains information of LOS acceleration of spacecraft and can infer small bodies' dynamic parameters such as the mass and gravity field while the spacecraft is flying by small bodies. In our Mars Express (MEX) tracking test case, the total LOS acceleration precision was about 1.5×10^{-6} m s^{-2} (0.15 mgal, under constraint of 20 dB of real tracking signal-to-noise ratio), which represents an improvement of about six times the magnitude over the traditional LOS acceleration approach. In our proposed method, a precise reference orbit is needed in theoretical LOS computation. The amount of computation for raw data reduction is very large. Instead of the implication of special computing equipment such as ASIC (Application Specific Integrated Circuit) used by the traditional Doppler process, we use a GPGPU (General Purpose Computing on Graphics Processing Unit) device to process LOS raw data. In this work, we use the NVIDIA company produced GTX580 graphic card which has 196 Gflops (double precision) computation ability to accelerate the computation. Every data block has 400 K raw data points and process time for one block is about 5 s. Real-time data processing could be achieved with faster professional computing cards such as Tesla K80.

This paper is arranged in this way: in Section 2 we introduce the raw data process and theoretical model of LOS acceleration. In Section 3 we describe the observation data and their error sources; in Section 4 we present a solution for Phobos mass and low degree and order gravity field coefficients. In Section 5 we present results and analysis based on the simulation of MEX Phobos flyby; and conclusions are drawn in Section 6.

2 MEASUREMENT AND THEORETICAL MODEL OF THE LOS ACCELERATION

This section introduces the zero-level tracking data process and force models considered in total LOS acceleration observation.

2.1 One-way Mode Data Processing

By ignoring orders higher than $\frac{1}{c^2}$ terms and gravitational delay effect, the relation of down-link frequency to spacecraft transponder frequency can be expressed as (Moyer 1971),

$$\begin{aligned}\frac{f_r}{f_t} =& 1 + \frac{1}{c}(\boldsymbol{v}_2 - \boldsymbol{v}_3)\cdot\boldsymbol{e}_{23} + \frac{1}{c^2}\left[(\boldsymbol{v}_2\cdot\boldsymbol{e}_{23})^2\right. \\ & - (\boldsymbol{v}_2\cdot\boldsymbol{e}_{23})(\boldsymbol{v}_3\cdot\boldsymbol{e}_{23}) + \frac{1}{2}(|\boldsymbol{v}_3|^2 - |\boldsymbol{v}_2|^2) \\ & \left. + (\phi_3 - \phi_2)\right] ,\end{aligned} \tag{1}$$

in which f_r is the received frequency of the down-link station, f_t is the transmitted frequency of spacecraft. The subscripts 2 and 3 denote the spacecraft and the down-link station, c is the speed of light, and $\boldsymbol{v_2}$ and $\boldsymbol{v_3}$ are the inertial velocity of spacecraft and the station relative to the Sun. $\boldsymbol{e_{23}}$ is the unit vector from the spacecraft to station; and ϕ_3 and ϕ_2 are the gravitational potential at down-link station and spacecraft position. Thus, the received frequency at the station can be written as

$$f_r = f_t\left(1 + \frac{v}{c}\right) + \delta\left(\frac{f_t}{c^2}\right) , \tag{2}$$

where v is the LOS velocity of the spacecraft relative to the ground station. The first term of Equation (2) shows the linear relationship between f_r and v. The second term is much smaller than the first one and has order of $\frac{f_t}{c^2}$. By differentiating Equation (2) the LOS acceleration (ignoring any variation of the transmitting frequency) can be expressed as

$$a_{\rm los} = \frac{dv}{dt} = \frac{c}{f_t}\frac{df_r}{dt} - \frac{c}{f_t}\frac{d}{dt}\left[\delta\left(\frac{f_t}{c^2}\right)\right] , \tag{3}$$

where t is the down-link station atomic time. The full expansion of Equation (3) can be found in supplementary material A. The observed LOS acceleration includes two terms. The first is relative to the variation of observed frequency and extracted from radio tracking data. The second term is relative to the differential of the higher order term mentioned in Equation (2). This term is added as a calibration factor in post processing. By ignoring the second term of Equation (2), the relation between the LOS acceleration and frequency derivative is expressed as

$$a_{\rm los} = \frac{c}{f_t}\frac{df_r}{dt} . \tag{4}$$

In the tracking data process, the typical raw data block span we use is 2 s. If the LOS acceleration is expanded linearly as

$$\tilde{a}_{\rm los} \approx k_1 + k_2 t . \tag{5}$$

The truncated error of Equation (4) is

$$|a_{\rm los} - \tilde{a}_{\rm los}| = \frac{h}{2}|\ddot{a}(\xi)|, \qquad \xi \in \{-1, 1\}\,. \tag{6}$$

Normally the second derivative of LOS acceleration is very small. Figure 1 shows the details of the second derivative of LOS acceleration variation near the flyby point. The maximum absolute value of $1.7 \times 10^{-6}\ \mathrm{m\,s^{-2}}$ in Figure 1 corresponds to the closest flyby time. From Equation (6) and Figure 1 we can see that during the MEX flyby Phobos the remaining error is no more than $8 \times 10^{-7}\ \mathrm{m\,s^{-2}}$. Because the observable precision of MEX is around $2 \times 10^{-6}\ \mathrm{m\,s^{-2}}$ and the maximum remaining error is smaller than the observable precision, a linear approximation as shown in Equation (5) is acceptable for computing LOS acceleration. In some other cases orders of Taylor series can be adapted to the magnitude of truncated error. From Equations (4) and (5), the deviation of the received frequency can be expressed linearly as

$$\frac{df(t)}{dt} = a + bt\,, \tag{7}$$

where a is the constant term at the data block center and b is the slope. Based on Equation (7), the signal frequency and phase within one data block are expressed as

$$\begin{aligned} f_r(t) =& c_4 + c_5 t + c_6 t^2\,, \\ \Phi(t) =& c_0 + c_1 t + c_2 t^2 + c_3 t^3\,. \end{aligned} \tag{8}$$

where

$$\begin{aligned} & f_r = \frac{d\Phi}{dt}\,, \\ & c_1 = c_4, \quad c_5 = 2c_2, \quad c_6 = 3c_3\,. \end{aligned} \tag{9}$$

Thus, the received signal $s(t)$ at a station can be written as:

$$s(t) = \mathrm{Amp} \times \cos(c_0 + c_1 t + c_2 t^2 + c_3 t^3)\,. \tag{10}$$

The coefficients $c_i (i = 0, 1, 2, 3)$ and amplitude are obtained by fitting Equation (10) to the narrow-band tracking signal. From Equations (4), (5) and (10) the LOS acceleration $a_{\rm los}$ of the spacecraft relative to the station is

$$a_{\rm los}(t) = -\frac{c}{f_t}(2c_2 + 6c_3 t)\,. \tag{11}$$

Our discrete LOS observable is defined as the acceleration at the block center

$$a_{\rm los} = -\frac{c}{f_t} 2c_2\,. \tag{12}$$

Of course, as each block is separately defined, we have to ensure that no large jumps of the LOS acceleration will occur from block to block. The jumps of LOS acceleration can be detected by the fitting coefficients which are related to each other. Thus, the jumps of acceleration can be detected by the discontinuity of modulo phase at the block border which is influenced by white noise and the polynomial truncation error expressed in Equation (6). Details of phase continuity can be found in the supplementary material B.

2.2 Two (three)-way Mode Data Processing

In two (three)-way tracking modes, the received frequency can be expressed as:

$$f_r = f_t M\Big(1 + \frac{v_{21} + v_{32}}{c}\Big) + \delta\Big(\frac{f_t}{c^2}\Big)\,, \tag{13}$$

and the corresponding frequency derivative is

$$\frac{df_r}{dt} = f_t M \frac{a_{\rm los}^{\rm up} + a_{\rm los}^{\rm down}}{c^2} + \frac{d}{dt}\delta\left(\frac{f_t}{c^2}\right)\,, \tag{14}$$

where M is the transponder ratio on spacecraft, $a_{\rm los}^{\rm up}$ is up-link LOS accelerations (up-link station to spacecraft) and $a_{\rm los}^{\rm down}$ is down-link LOS accelerations (spacecraft to down-link station), and $a_{\rm los}^{\rm total}$ is the total acceleration which is expressed as

$$a_{\rm los}^{\rm total} = \frac{c}{f_t M}\frac{df_r}{dt} - \frac{c}{f_t M}\frac{d}{dt}\Big[\delta\Big(\frac{f_t}{c^2}\Big)\Big]\,. \tag{15}$$

The tracking data process of two (three)-way mode is the same as one-way mode. The first term of Equation (14) is extracted from tracking data and the second term added in the post process as calibration factor will be discussed in Section 3.

2.3 Computation of the Theoretical LOS Acceleration

To illustrate our approach, we consider an MEX Phobos flyby case. The acceleration of the spacecraft relative to the down-link station is

$$\boldsymbol{a}_{\rm sta^3 sat^2} = \boldsymbol{a}_{\rm sat^2} - \boldsymbol{a}_{\rm sta^3}\,. \tag{16}$$

For discussion convenience mark 2 indicates the time of signal transmission by spacecraft and 3 defines the receiving time at the down-link station. In Equation (16) $\boldsymbol{a}_{\rm sat^2}$ is the acceleration of the spacecraft relative to SSB (solar system barycenter) at the signal transmission time. $\boldsymbol{a}_{\rm sta^3}$ is the acceleration of the station relative to SSB at the receiving time. The J2000 coordinate system is employed for $\boldsymbol{a}_{\mathbf{sat^2}}$ and $\boldsymbol{a}_{\rm sta^3}$. If introducing intermediate objects, such as Mars and the Earth into Equation (16), it becomes

$$\begin{aligned}\boldsymbol{a}_{\mathrm{sta}^3\mathrm{sat}^2} &= \boldsymbol{a}_{\mathrm{sat}^2} - \boldsymbol{a}_{\mathrm{sta}^3} \\ &= \boldsymbol{a}_{\mathrm{Mars}^2} + \boldsymbol{a}_{\mathrm{Mars}^2\mathrm{sat}^2} - (\boldsymbol{a}_{\oplus^3} + \boldsymbol{a}_{\oplus^3\mathrm{sta}^3}) \\ &= \boldsymbol{a}_{\mathrm{Mars}^2\mathrm{sat}^2} + \boldsymbol{a}_{\oplus^3\mathrm{Mars}^2} - \boldsymbol{a}_{\oplus^3\mathrm{sta}^3} \ .\end{aligned} \tag{17}$$

In Equation (17) $\oplus$ denotes Earth and $Mars$ is Mars. The equation shows that the acceleration of a spacecraft relative to station includes three parts: the first is the acceleration of spacecraft relative to Mars mass center; the second is the acceleration of Mars mass center relative to the Earth mass center; and the third part is the acceleration of the station relative to Earth. The first part of Equation (17) is expressed as

$$\begin{aligned}\boldsymbol{a}_{\mathrm{Mars}^2\mathrm{sat}^2} =& \boldsymbol{a}^{\mathrm{Mars}}_{\mathrm{twobody}} + \boldsymbol{a}_{PM} + M^{\mathrm{Mars}}_{N,J,\psi,I,\phi}\Delta U_{\mathrm{Mars}} \\ &+ M^{\mathrm{Phobos}}_{\alpha,\beta,w}\Delta U_{\mathrm{Phobos}} + \boldsymbol{a}_{\mathrm{srp}} \ ,\end{aligned} \tag{18}$$

in which the right-hand terms represent the two-body acceleration (time reference is 2) by central body Mars, the third body perturbation by other planets, the gravity acceleration by Mars non-sphere gravity field, the Phobos second order gravity acceleration, and acceleration by solar radiation pressure, respectively. In Equation (18) $M^{\mathrm{Mars}}_{N,J,\psi,I,\phi}$ is a transformation matrix between Mars-fixed coordinates to inertial coordinates given by Konopliv et al. (2006), and U_{Mars} is Mars gravity field potential. Using five parameters Folkner et al. (1997) define the transformation matrix. The MRO110c model was selected as Martian gravity model (*http://pds-geosciences.wustl.edu/mro/mro-m-rss-5-sdp-v1/mrors_1xxx/data/shadr/*). $M^{\mathrm{Phobos}}_{\alpha,\beta,\omega}$ is the IAU-defined transformation matrix from Phobos-fixed coordinates to J2000 inertial coordinates system (Archinal et al. 2011). The coefficients α and β are the right ascension and declination of the north pole of Phobos relative to the J2000 frame, and w specifies the ephemeris position of the prime meridians. The conversion from a Phobos-fixed coordinate system to J2000 inertial coordinate system is shown in Figure 2. The final term in Equation (18) is the solar radiation pressure (SRP). Because no detailed information about the optical properties of the spacecraft is available, a simple SRP model as shown in Equation (19) Andert et al. (2010) was used

$$\boldsymbol{a}_{\mathrm{srp}} = -k\frac{q_{\mathrm{s}}}{c}\frac{r_0^2}{r_{\odot}^2}\frac{A_{\mathrm{exp}}}{m_{\mathrm{sc}}}\boldsymbol{e}_{\odot} \ . \tag{19}$$

It is assumed that the normal solar array surface direction always points in the direction of the Sun, while k is a scaling factor which accounts for the variation of solar flux, q_{s} is the solar flux at 1 AU distance which is about 1367 W m^{-2}, c is the speed of light, r_0 is the distance of 1 AU, and $r_{\odot}$ is the distance from the Sun to the spacecraft. The value $\frac{A_{\mathrm{exp}}}{m_{\mathrm{sc}}}$ is the area-mass ratio of the spacecraft and $\boldsymbol{e}_{\odot}$ is the unit vector in the direction of the Sun. In parameter estimation, $k\frac{A_{\mathrm{exp}}}{m_{\mathrm{sc}}}$ is set as one parameter to be solved. Because the Martian atmosphere is extremely thin and the height of Phobos flyby was about 6000 km to the surface of Mars, atmosphere drag force is ignored.

The second part of Equation (17) is the acceleration of Mars to Earth. A simple way to compute this term is to differentiate the velocity of Mars to the Earth from ephemeris, however, the precision is not guaranteed. A direct approach with higher precision computes the gravitational acceleration of Mars and Earth in the SSB reference frame (Moyer 1971) is

$$\begin{aligned}&\boldsymbol{a}_{\oplus^3\mathrm{Mars}^2} = \boldsymbol{a}_{\mathrm{Mars}^2} - \boldsymbol{a}_{\oplus^3} \\ =&\sum_{\substack{i=1\\ i\neq 4}}^{10}\frac{GM_i}{|\boldsymbol{r}_{\mathrm{Mars},i}|^2}\frac{\boldsymbol{r}_{\mathrm{Mars},i}}{|\boldsymbol{r}_{\mathrm{Mars},i}|} + \sum_{j=1}^{2}\frac{GM_j}{|\boldsymbol{r}_{\mathrm{Mars},j}|^2}\frac{\boldsymbol{r}_{\mathrm{Mars},j}}{|\boldsymbol{r}_{\mathrm{Mars},j}|} \\ &- \left[\sum_{\substack{i=1\\ i\neq 3}}^{10}\frac{GM_i}{|\boldsymbol{r}_{\oplus,i}|^2}\frac{\boldsymbol{r}_{\oplus,i}}{|\boldsymbol{r}_{\oplus,i}|} + \frac{GM_{\mathrm{Moon}}}{|\boldsymbol{r}_{\oplus,\mathrm{Moon}}|^2}\frac{\boldsymbol{r}_{\oplus,\mathrm{Moon}}}{|\boldsymbol{r}_{\oplus,\mathrm{Moon}}|}\right] \ .\end{aligned} \tag{20}$$

In Equation (20) $\boldsymbol{r}_{\mathrm{Mars},i}$ is the coordinate vector from Martian mass center to the ith planet in the solar system. The value $\boldsymbol{r}_{\oplus,i}$ is the coordinate vector from the Earth mass barycenter to the ith planet in the solar system. The mark j denotes the two Martian satellites, Phobos and Deimos. Because we consider the mass center of Mars and the Earth rather than their system barycenter, the influence of the Martian satellite and the Earth satellite are considered separately.

The third part of Equation (17) is the acceleration of the station relative to the Earth mass center in the J2000 frame. Considering the transformation of the station coordinates from an earth body fixed frame to the J2000 frame

$$\boldsymbol{r}_{\mathrm{j2000(sta}^3)} = M_{[\mathrm{itrf}-\mathrm{icrf}]}\boldsymbol{r}_{\mathrm{fixed(sat}^3)} \ , \tag{21}$$

in which $M_{[\mathrm{itrf}-\mathrm{icrf}]}$ is the transformation matrix from Earth body-fixed frame to the J2000 frame at the signal receiving time including precession, nutation, rotation, and polar motion, and $\boldsymbol{r}_{\mathrm{j2000(sta}^3)}$ is the coordinate vector from the Earth center to the station in the J2000 frame and $\boldsymbol{r}_{\mathrm{fixed(sat}^3)}$ is the geocentric coordinate of station. Ignoring tidal influence the corresponding acceleration of station relative to the Earth mass center is

$$\boldsymbol{a}_{\oplus^3\mathrm{sta}^3} = \frac{d^2M(t)}{dt^2}\boldsymbol{r}_{\mathrm{fixd(sta^3)}} \ . \tag{22}$$

By combining Equations (18), (19), (20) and (22) with Equation (17) the theoretical one-way LOS acceleration can be written as

$$\begin{aligned} a_{\mathrm{los}} =& \boldsymbol{a}_{\mathrm{sta^3sat^2}} \cdot \frac{\boldsymbol{r}_{sat^2} - \boldsymbol{r}_{\mathrm{sta}^3}}{|\boldsymbol{r}_{\mathrm{sat}^2} - \boldsymbol{r}_{\mathrm{sta}^3}|} \\ =& \Big[\boldsymbol{a}^{\mathrm{Mars}}_{\mathrm{twobody}} + \boldsymbol{a}_{PM} + M^{\mathrm{Mars}}_{N,J,\psi,I,\phi}\Delta U_{\mathrm{Mars}} + M^{\mathrm{Phobos}}_{\alpha,\beta,w}\Delta U_{\mathrm{Phobos}} + \boldsymbol{a}_{\mathrm{srp}} \\ &+ \sum_{\substack{i=1\\ i\neq 4}}^{10} \frac{GM_i}{|\boldsymbol{r}_{\mathrm{Mars},i}|^2}\frac{\boldsymbol{r}_{\mathrm{Mars},i}}{|\boldsymbol{r}_{\mathrm{Mars},i}|} + \sum_{j=1}^{2} \frac{GM_j}{|\boldsymbol{r}_{\mathrm{Mars},j}|^2}\frac{\boldsymbol{r}_{\mathrm{Mars},j}}{|\boldsymbol{r}_{\mathrm{Mars},j}|} - \left(\sum_{\substack{i=1\\ i\neq 3}}^{10} \frac{GM_i}{|\boldsymbol{r}_{\oplus,i}|^2}\frac{\boldsymbol{r}_{\oplus,i}}{|\boldsymbol{r}_{\oplus,i}|} + \frac{GM_{\mathrm{Moon}}}{|\boldsymbol{r}_{\oplus,\mathrm{Moon}}|^2}\frac{\boldsymbol{r}_{\oplus,\mathrm{Moon}}}{|\boldsymbol{r}_{\oplus,\mathrm{Moon}}|}\right) \\ &- \frac{d^2M(t)}{dt^2}\boldsymbol{r}_{\mathrm{fixd(sta^3)}}\Big] \cdot \boldsymbol{e}_{\mathrm{los}} \ , \end{aligned} \tag{23}$$

where vector $\boldsymbol{e}_{\mathrm{los}} = \frac{\boldsymbol{r}_{\mathrm{sat}^2} - \boldsymbol{r}_{\mathrm{sta}^3}}{|\boldsymbol{r}_{sat^2} - \boldsymbol{r}_{\mathrm{sta}^3}|}$ define the vector of LOS direction from down-link station to spacecraft. Corresponding two (three)-way LOS accelerations can be written as (up-link part)

$$\begin{aligned} a^{\mathrm{up}}_{\mathrm{los}} =& \boldsymbol{a}_{\mathrm{sat^2sta^1}} \cdot \frac{\boldsymbol{r}_{\mathrm{sta}^1} - \boldsymbol{r}_{sat^2}}{|\boldsymbol{r}_{\mathrm{sta}^1} - \boldsymbol{r}_{\mathrm{sat}^2}|} = \Big[\frac{d^2M(t)}{dt^2}\boldsymbol{r}_{\mathrm{fixd(sta^3)}} + \\ &\sum_{\substack{i=1\\ i\neq 3}}^{10} \frac{GM_i}{|\boldsymbol{r}_{\oplus,i}|^2}\frac{\boldsymbol{r}_{\oplus,i}}{|\boldsymbol{r}_{\oplus,i}|} + \frac{GM_{\mathrm{Moon}}}{|\boldsymbol{r}_{\oplus,\mathrm{Moon}}|^2}\frac{\boldsymbol{r}_{\oplus,\mathrm{Moon}}}{|\boldsymbol{r}_{\oplus,\mathrm{Moon}}|} - \left(\sum_{\substack{i=1\\ i\neq 4}}^{10} \frac{GM_i}{|\boldsymbol{r}_{\mathrm{Mars},i}|^2}\frac{\boldsymbol{r}_{\mathrm{Mars},i}}{|\boldsymbol{r}_{\mathrm{Mars},i}|} + \sum_{j=1}^{2} \frac{GM_j}{|\boldsymbol{r}_{\mathrm{Mars},j}|^2}\frac{\boldsymbol{r}_{\mathrm{Mars},j}}{|\boldsymbol{r}_{\mathrm{Mars},j}|}\right) \\ &- (\boldsymbol{a}^{\mathrm{Mars}}_{\mathrm{twobody}} + \boldsymbol{a}_{PM} + M^{\mathrm{Mars}}_{N,J,\psi,I,\phi}\Delta U_{\mathrm{Mars}} + M^{\mathrm{Phobos}}_{\alpha,\beta,w}\Delta U_{\mathrm{Phobos}} + \boldsymbol{a}_{\mathrm{srp}})\Big] \cdot \boldsymbol{e}^{\mathrm{up}}_{\mathrm{los}} \ , \end{aligned} \tag{24}$$

and the down-link part (same as one way)

$$\begin{aligned} a^{\mathrm{down}}_{\mathrm{los}} =& \boldsymbol{a}_{\mathrm{sta^3sat^2}} \cdot \frac{\boldsymbol{r}_{\mathrm{sat}^2} - \boldsymbol{r}_{\mathrm{sta}^3}}{|\boldsymbol{r}_{\mathrm{sat}^2} - \boldsymbol{r}_{\mathrm{sta}^3}|} \\ =& \big[\boldsymbol{a}^{\mathrm{Mars}}_{\mathrm{twobody}} + \boldsymbol{a}_{PM} + M^{\mathrm{Mars}}_{N,J,\psi,I,\phi}\Delta U_{\mathrm{Mars}} + M^{\mathrm{Phobos}}_{\alpha,\beta,w}\Delta U_{\mathrm{Phobos}} + \boldsymbol{a}_{\mathrm{srp}} + \\ &\sum_{\substack{i=1\\ i\neq 4}}^{10} \frac{GM_i}{|\boldsymbol{r}_{\mathrm{Mars},i}|^2}\frac{\boldsymbol{r}_{\mathrm{Mars},i}}{|\boldsymbol{r}_{\mathrm{Mars},i}|} + \sum_{j=1}^{2} \frac{GM_j}{|\boldsymbol{r}_{\mathrm{Mars},j}|^2}\frac{\boldsymbol{r}_{\mathrm{Mars},j}}{|\boldsymbol{r}_{\mathrm{Mars},j}|} - \left(\sum_{\substack{i=1\\ i\neq 3}}^{10} \frac{GM_i}{|\boldsymbol{r}_{\oplus,i}|^2}\frac{\boldsymbol{r}_{\oplus,i}}{|\boldsymbol{r}_{\oplus,i}|} + \frac{GM_{\mathrm{Moon}}}{|\boldsymbol{r}_{\oplus,\mathrm{Moon}}|^2}\frac{\boldsymbol{r}_{\oplus,\mathrm{Moon}}}{|\boldsymbol{r}_{\oplus,\mathrm{Moon}}|}\right) \\ &- \frac{d^2M(t)}{dt^2}\boldsymbol{r}_{\mathrm{fixd(sta^3)}}\Big] \cdot \boldsymbol{e}^{\mathrm{down}}_{\mathrm{los}} \ . \end{aligned} \tag{25}$$

In Equation (23), the direction of the unit LOS vector is from the up-link station to the spacecraft, while in Equation (25) the direction of unit LOS vector is from the spacecraft to down-link station. In the present work, we did not include small perturbations such as the Martian tidal force and general relativity. These force models are the topic of future work.

3 TRACKING DATA SIMULATION AND PROCESSION

On 2013 December 29, MEX conducted a flyby of Phobos at a minimum distance of 58 km. This distance was the closest with respect to previous flybys (459 km for the flyby on 2006 March 23 and 275 km on 2008 July 17, respectively). In tracking data simulation Chinese VLBI (Very Long Baseline Interferometry) Sheshan station near Shanghai is the receiving station and New Norcia ESA station is the up-link station. The receiving frequency is approximately 8420.15 MHz. The signal-to-noise ratio is about 20 dB. The formula applied in the raw data simulation process is

$$\begin{aligned} \phi(t) =& \int_{t_0}^{t} \left[f_t M\Big(1 + \frac{v_{21} + v_{32}}{c}\Big) + \delta\Big(\frac{f_t}{c^2}\Big)\right] ds \ , \\ S(t) =& \mathrm{Amp}\cos[\phi(t) + \phi_0] + \mathcal{N}(\mu,\, \sigma^2) \ . \end{aligned} \tag{26}$$

In this formula $\phi(t)$ is the received signal phase of the down-link station, f_t is the transmission frequency of up-link station with a value of 7166.69 MHz, and M is the transponder ratio onboard MEX which value is 880/749 at X band, and v_{21} is the LOS velocity of the up-link station relative to MEX and v_{32} is the velocity of Mex relative to down-link station (all the velocities are from the recovered orbit of MEX); $\delta(\frac{f_t}{c^2})$ is the second term introduced in Equation (2). $S(t)$ is the simulated signal. The initial phase ϕ_0 is set to zero. The amplitude of the signal is set as the real tracking signal level at the elevation of 20 degrees ignoring amplitude variation. $\mathcal{N}(\mu, \sigma^2)$ is white noise with $\mu = 0$ and $\sigma \simeq 20$ dB. Raw data sampling rate is set to 200 kHz.

The differential evolution (DE) algorithm is used in raw data reduction. We have tried this algorithm for Doppler extraction in an earlier Chinese Lunar mission (Jian et al. 2009). The DE algorithm is a global optimization estimator and is designed to solve nonlinear problems. There are two reasons to select the DE algorithm for parameters estimation in LOS observable computation. Firstly, the driver of the DE algorithm can be paralleled coded that is feasibility in huge raw data processing; Secondly, the performance of the DE algorithm has good stable convergence success used in these kinds of applications (Price et al. 2006). Detail information can be found at the website (*http://www1.icsi.berkeley.edu/ storn/code.html*). The down-link signal in tracking data block (2 s) can be expanded at block center as (mentioned in Eq. (10))

$$\begin{aligned}\tilde{S}(t) =&(c_4 + c_5 t)\cos(c_0 + c_1 t + c_2 t^2 + c_3 t^3) \\ &+ \mathcal{N}(\mu, \sigma^2) \ .\end{aligned} \tag{27}$$

where c_0 to c_3 are the coefficients of Taylor polynomial from the expansion of signal phase. c_4 and c_5 are the amplitude with linear slope. The slope is not considered in our simulation but in real data procession would be considered. The objective function in DE fitting process is defined as

$$\chi_{\min} = \sum_{i=1}^{4\times10^5} [S(i) - \tilde{S}(i)]^2 \ . \tag{28}$$

After raw data reduction we can get the coefficients which can be used to form the LOS observables. We use GPGPU to accelerate the computation speed. The computation speed is increased by $4 \sim 5$ times compared with an Intel E5-2620 platform with eight kernels. One data block procession time is about 5 s. It needs to be noted that during our observation simulation, we do not make use of a priori Phobos gravity field information. We only use the MEX precise ephemeris to generate the observation through Equation (26). Thus, it is possible to retrieve Phobos gravity information to validate the effectiveness of this algorithm.

Table 1 The a Priori Values of the Parameters

Parameter	Value	Reference
$GM_{\rm Phobos}$	708754 $\rm m^3\ s^{-2}$	Acton (1996)
R_0	11270 m	Willner et al. (2010)
C_{20}	–0.05121	Pätzold et al. (2014)
C_{22}	0.00387	Pätzold et al. (2014)

4 SOLUTION OF THE MASS AND GRAVITATIONAL FIELD OF SMALL CELESTIAL BODIES

The parameters to be solved included $GM_{\rm Phobos}$ (product of the gravitational constant and the mass) and low degree gravity field coefficients of a small body. The observation Equation (21) is written in a parametric form as

$$\begin{aligned}a_{\rm los} =&\big[M^{\rm Phobos}_{\alpha,\beta,w}\boldsymbol{F}(GM_{\rm Phobos}, \overline{C}_{nm}, \overline{S}_{nm}) \\ &+ \boldsymbol{F}_{\rm others}\big] \cdot \boldsymbol{e}_{\rm los} \ ,\end{aligned} \tag{29}$$

where $\boldsymbol{F}(GM_{\rm Phobos}, \overline{C}_{nm}, \overline{S}_{nm})$ is the Phobos gravity acceleration, and $\boldsymbol{F}_{\rm others}$ includes the effect of all other forces but the gravity of Phobos. The parameters $GM_{\rm Phobos}, \overline{C}_{nm}, \overline{S}_{nm}$ are solved using conventional least-square method with a proper linearization.

In our computation the inertial ellipsoidal coordinates of Phobos were used, and the non-zero gravity field coefficients to be solved were $\overline{C}_{20}$ and $\overline{C}_{22}$ (Andert et al. 2010).

5 RESULTS AND ANALYSIS

All the external forces acting on the spacecraft during the flyby are summarized in Figure 3. At the nearest point, the Phobos gravity reached a magnitude of 10^{-4} $\rm m\ s^{-2}$. Among these items, the perturbation of the Sun, the solar radiation pressure (SRP) and the Phobos gravity field are at the same order of magnitude.

The observation geometry is given in Figure 4. When the spacecraft velocity is perpendicular to the LOS, no information about the dynamic state of the spacecraft carried over to the LOS acceleration. During the flyby we were close to a very favorable edge-on orbit.

In Table 1 we give the a priori values for the parameters solved in this paper. As we have mentioned, the observation we simulated does not make use of Phobos gravity field information. The values in Table 1 are used as the initial value in our inversion. Thus, the retrieved Phobos gravity field results can be compared with current publications.

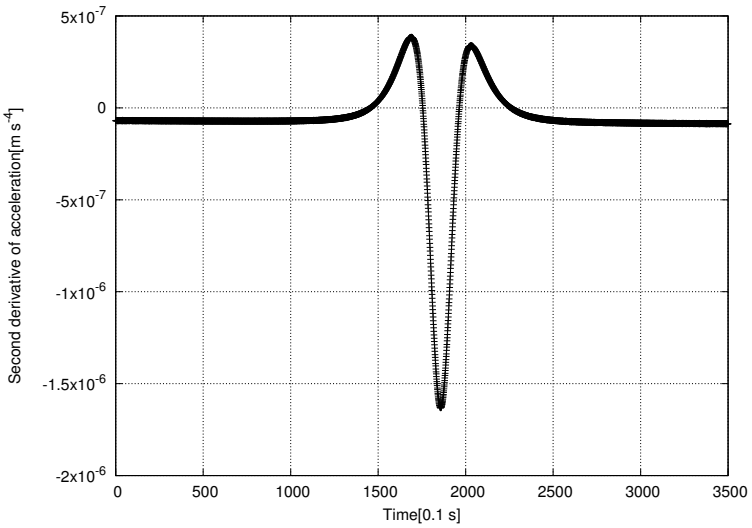

Fig. 1 Second derivative of LOS acceleration of MEX relative to Shanghai station near flyby point (time interval is 0.1 s and time span is about 5 min).

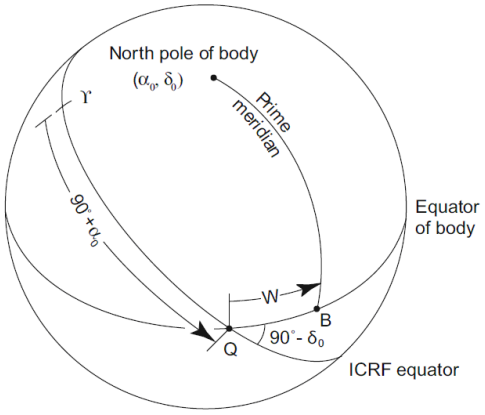

Fig. 2 The transformation between a Phobos-fixed coordinate system to an inertial coordinate system (Archinal et al. 2011).

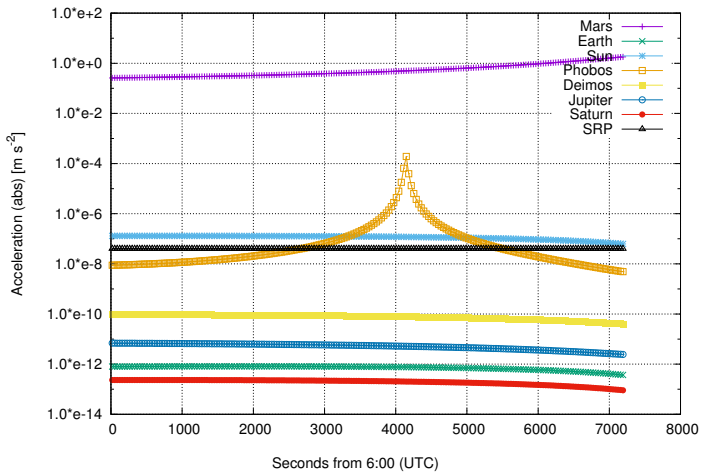

Fig. 3 The variation of all the external forces acting on the MEX spacecraft during the flyby. The major forces are the Martian gravity field, the three-body perturbation of the Sun, the solar radiation pressure, and the gravity of Phobos.

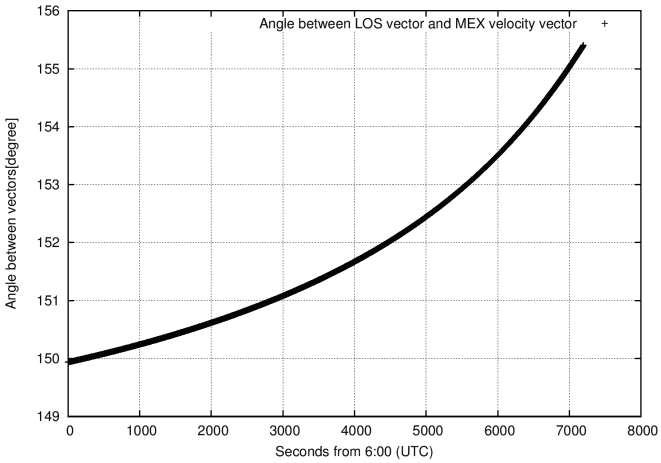

Fig. 4 Angle variation during the flyby between the MEX spacecraft velocity and the LOS acceleration.

The standard deviation of the LOS observation data was $1.5 \times 10^{-6}\ \mathrm{m\ s^{-2}}$ based on data processing (we obtained the value of the noise standard deviation by removing the trend term in the observations). The distribution of the LOS residuals after least square fitting is shown in Figure 5.

In Figure 5 we give the LOS acceleration residuals after parameter solution. About the first 1000 s. we have a chance to track the MEX and generate the LOS observation. However, it is impossible to estimate gravitational parameters of Phobos using such short time tracking data. In order to make the computation consistent, and as the object of this work is to validate the effectiveness of this new tracking method, we do the computation only using simulated data. The first 1000 s observation are also used to verify the simulation data.

From Figure 5 we can see that the significant improvement in the LOS residuals after we considered the influence of the Phobos mass and degree two gravity field coefficients step by step. The difference between the RMS of the LOS residuals with and without estimation of the degree two gravity field coefficients is not significant; however, from the bottom plot in Figure 5 we can see a clear reduction around the nearest point in the residuals for the flyby after we estimated the degree two coefficients.

In Tables 2 and 3 we present various estimates of Phobos mass and degree two gravity coefficients. Table 2 shows that our estimate is close to the most recent value calculated by Pätzold et al. (2014).

From Table 2 we find that our GM value result is consistent with those from Andert et al. (2010) and Pätzold et al. (2014). The reason is that both of these works use the flyby tracking data of MEX, even though they use Doppler tracking data; in our work we use total LOS acceleration generated from the MEX precise ephemeris. Compared with results from Andert et al. (2010) and Pätzold et al. (2014), our results show better formal accuracy. This may be related to the high accuracy of the LOS acceleration data ($1.5 \times 10^{-6}\ \mathrm{m\ s^{-2}}$). Another potential reason is that the flyby distance of 58 km in our computation is shorter than the flyby distance 275 km applied in their work. In addition, the relative error and uncertainty of the GM value in our result (with gravity solved) is in the same level as those of Jacobson (2010 without gravity solved). The comparison indicates the potential advantage of LOS acceleration method to the traditional Doppler method.

In Table 3 we can see that our solution of $\overline{C}_{20}$ and $\overline{C}_{22}$ is consistent with those of Pätzold et al. (2014) and within the error range. Because of the shorter flyby distance and high accuracy of the LOS acceleration data we used in this work, we find that the formal error of $\overline{C}_{20}$ has an improvement of about a factor of five. As the time length of flyby data is limited, the improvement of $\overline{C}_{22}$ is not significant. Even though we retrieve the gravity field parameters from the simulated data instead of real tracking data, the consistent values with recent published values, and the improved formal errors indicate the reliability of our proposed total LOS acceleration method. The relatively low formal error from our method as presented in Table 3 probably has three reasons. The first is the signal to noise level of simulated raw data (Eq. (26)) which is about 20 dB from the real tracking data. The second is the different raw data process algorithms of the LOS method (Taylor series fitting) and the conventional Doppler (phase counting). The third is that the flyby distance 58 km in our computation is shorter than the former distance that the Doppler method adopted.

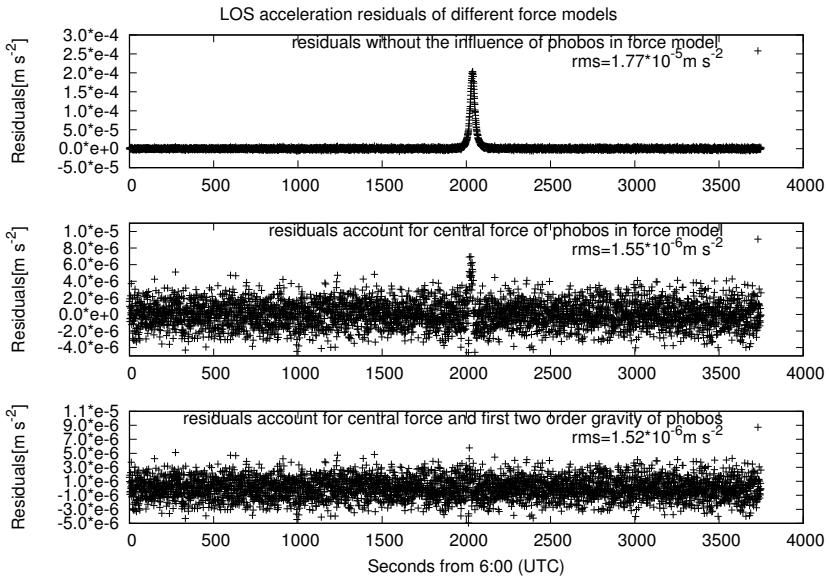

Fig. 5 Distributions of the LOS acceleration residuals after the least squares fits. In the top plot, the central gravitation and gravitational field of Phobos are not considered; in the middle plot the central gravitation of Phobos is considered while the degree two gravity field is not included; and in the bottom plot both the central gravitation and degree two gravity field are considered. The sampling gap is 2 s.

Table 2 Several Estimates of the GM Value of Phobos from Various Flybys

Data base	GM value (10^{-4} km^3 s^{-2})	Relative error	Reference
Viking	6.600± 0.8	12.1	Christensen et al. (1977)
Viking	7.300± 0.7	9.5	Tolson et al. (1977)
Viking	8.500± 0.7	8.2	Williams et al. (1988)
Phobos-2	7.220± 0.05	0.7	Kolyuka et al. (1990)
Phobos-2	7.163± 0.008	0.1	Berthias (1990)
Viking only	7.126± 0.045	0.6	Jacobson (2010)
Viking only(w/o non-grav.accel.)	7.077± 0.003	0.04	Jacobson (2010)
Phobos-2 only	7.091± 0.005	0.07	Jacobson (2010)
Phobos-2 only (w/o non-grav. accel.)	7.091± 0.005	0.07	Jacobson (2010)
Viking & Phobos-2 combined	7.092± 0.004	0.06	Jacobson (2010)
Mars Express 2006	7.120± 0.120	1.70	Andert et al. (2010)
Mars Express 2008 (UniBw)	7.127± 0.021	0.30	Andert et al. (2010)
Mars Express 2010 (with C_{20})	7.072± 0.014	0.20	Pätzold et al. (2014)
Mars Express 2010 (GM only)	7.084± 0.007	0.10	Pätzold et al. (2014)
Mars Express 2013 (with C20, C22)	7.088± 0.003	0.04	This paper

Table 3 The Degree Two Gravity Coefficient Estimates of Phobos

Data base	$\overline{C}_{20}$	$\overline{C}_{22}$	Reference
MEX flyby 2010 (Doppler)	–0.0512± 0.0651	0.0038±0.0086	Pätzold et al. (2014)
MEX flyby 2013 (LOS acceleration)	–0.0388± 0.0122	0.0124±0.0068	This paper

6 CONCLUSIONS

In this paper, we propose a method, the total LOS acceleration method, to obtain and model LOS acceleration observable from narrow-band tracking data which is different from the traditional LOS acceleration method. Compared to the conventional Doppler method of computing average velocity the LOS method trys to recover instantaneous line of sight acceleration which is useful in some tracking case such as flying by (hyperbolic orbit) and near perigee (elliptical orbit) with rapid change of velocity. We illustrated its feasibility by modeling the second degree and order gravity field of Phobos from a simulation arc during an MEX flyby that took place on 2013 December 29. Our GM value

result is consistent with those of Andert et al. (2010) and Pätzold et al. (2014) , and the values of $\overline{C}_{20}$ and $\overline{C}_{22}$ are also consistent with Pätzold et al. (2014) within error bar.

Our experiment validates the reliability of the total LOS acceleration method in planetary gravity field estimation. This method has the potential to be combined with theoretical analysis for future planetary and asteroid exploration (Hu & Ji 2017; Hu et al. 2015; Matsuoka & Russell 2017; Lauretta et al. 2017). It is also possible to reprocess the radio tracking data of Toutatis to study its mass information by employing this method Huang et al. (2013) and such a work will provide reference for Chinese asteroid exploration missions. Currently we have implemented this tracking mode for Mars and lunar spacecraft, and plan to process this datum in our independent Mars spacecraft precise orbit determination software MAGREAS (Yan et al. 2017). We will track lunar and Mars spacecraft with 65 m antenna at Shanghai to apply this method in real data processing. This method will hopefully be applied in other planetary exploration missions investigating planetary or asteroid gravity fields.

Acknowledgements We thank Mr. Gou Wei, from the Shanghai Sheshan Observatory for the MEX observation and Prof. Meng Qiao and Prof. Chen Congyan in Southeast University for advice on the data preprocessing. We thank Dr. ShangKun for his help on ancillary data. This work is supported by the National Natural Science Foundation of China (Nos. U1531136, U1831132 and U1531104), Innovation Group of Natural Fund of Hubei Province (2018CFA087), Open Funding of Macau University of Science and Technology (FDCT 119/2017/A3), and Open Funding of Guizhou Provincial Key Laboratory of Radio Astronomy and Data Processing (KF201813). We thank the European Space Agency for the permission to track the Mars Express spacecraft from the Shanghai Deep Space antenna.

References

Acton, C. H. 1996, Planet. Space Sci., 44, 65

Andert, T., Rosenblatt, P., Pätzold, M., et al. 2010, Geophysical Research Letters, 37

Archinal, B. A., A'Hearn, M. F., Bowell, E., et al. 2011, Celestial Mechanics and Dynamical Astronomy, 109, 101

Barriot, J. P., & Balmino, G. 1992, Icarus, 99, 202

Berthias, J. 1990, JPL IOM, 314

Christensen, E. J., Born, G. H., Hildebrand, C. E., & Williams, B. G. 1977, Geophys. Res. Lett., 4, 555

Folkner, W. M., Yoder, C. F., Yuan, D. N., Standish, E. M., & Preston, R. A. 1997, Science, 278, 1749

Han, S.-C. 2008, Journal of Geophysical Research (Planets), 113, E11012

Hu, S.-C., & Ji, J.-H. 2017, RAA (Research in Astronomy and Astrophysics), 17, 120

Hu, S.-C., Ji, J.-H., & Zhao, Y.-H. 2015, RAA (Research in Astronomy and Astrophysics), 15, 896

Huang, J., Ji, J., Ye, P., et al. 2013, Scientific Reports, 3, 3411

Jacobson, R. A. 2010, AJ, 139, 668

Jian, N., Shang, K., Zhang, S., et al. 2009, Science in China: Physics, Mechanics and Astronomy, 52, 1849

Kolyuka, Y. F., Ephimov, A. E., Kudryavtsev, S. M., et al. 1990, Pisma v Astronomicheskii Zhurnal, 16, 396

Konopliv, A. S., Yoder, C. F., Standish, E. M., Yuan, D.-N., & Sjogren, W. L. 2006, Icarus, 182, 23

Lauretta, D. S., Balram-Knutson, S. S., Beshore, E., et al. 2017, Space Sci. Rev., 212, 925

Matsuoka, A., & Russell, C. T. 2017, Space Sci. Rev., 208, 1

Moyer, T. D. 1971, Mathematical Formulation of the Double-Precision Orbit Determination Program (DPODP). (NASA, Jet Propulsion Lab., California Inst. Technology, Pasadena, California. Techn. Report 32-1527)

Muller, P. M., & Sjogren, W. L. 1968, Science, 161, 680

Pätzold, M., Andert, T. P., Tyler, G. L., et al. 2014, Icarus, 229, 92

Price, K., Storn, R. M., & Lampinen, J. A. 2006, Differential Evolution: a Practical Approach to Global Optimization (Springer Science & Business Media)

Sugano, T., & Heki, K. 2004, Geophys. Res. Lett., 31, L24703

Sun, X., Fei, L. I., Yan, J., & Hao, W. 2013, Geomatics & Information Science of Wuhan University, 38, 1430

Tolson, R. H., Blackshear, W. T., Mason, M. L., & Kelly, G. M. 1977, Geophys. Res. Lett., 4, 551

Williams, B., Duxbury, T., & Hildebrand, C. 1988, in Lunar and Planetary Science Conference, 19

Willner, K., Oberst, J., Hussmann, H., et al. 2010, Earth and Planetary Science Letters, 294, 541

Yan, J., Yang, X., Ye, M., et al. 2017, Ap&SS, 362, 123